

# **Autonomous Magnetized Cryo-Couplers with Active Alignment Control for Propellant Transfer (AMCC-AAC)**

**2025 Human Lander Challenge (HuLC) Proposal**

## **The Ohio State University**

Max Heil (Undergraduate, Aerospace Engineering)

Rahul Ravishankar (Undergraduate, Aerospace Engineering)

Will Rueter (Undergraduate, Aerospace Engineering)

Kevin Subin (Undergraduate, Aerospace Engineering)

Zafar Shaik (Undergraduate, Aerospace Engineering)

Nishanth Kunchala (Undergraduate, Aerospace Engineering)

Anastasia Anikina (Undergraduate, Aerospace Engineering)

Ryan Endicott (Undergraduate, Aerospace Engineering)

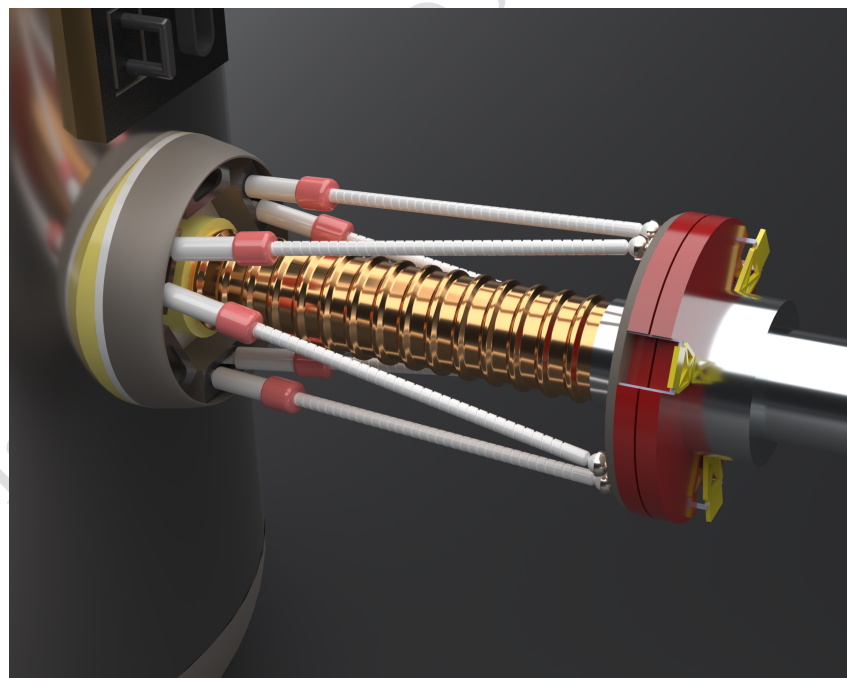
Artur Leonel Machado Ulsenheimer (Undergraduate, Aerospace Engineering)

Allie Renshaw (Undergraduate, Aerospace Engineering)

Shiv Amin (Undergraduate, Aerospace Engineering)

Tejdeep Somi Reddy (Undergraduate, Aerospace Engineering)

**Advisor:** Dr. John Horack



**Faculty Advisor Signature:** \_\_\_\_\_

© 2025 Max Heil - OSU HuLC Team  
Distribution Unlimited.

This proposal is a work in progress. No commitments or solicitations have been made by the authors to the reader. For use of any part of this proposal in future work, we kindly ask that you give proper credit to the authors. Please contact Max Heil at [heil.115@osu.edu](mailto:heil.115@osu.edu) for any comments/concerns.

## Contents

<b>1 Executive Summary</b>	<b>4</b>
<b>2 Problem Statement and NASA Relevance</b>	<b>4</b>
<b>3 Proposed Solution and Technical Approach</b>	<b>4</b>
3.1 Main Assumptions . . . . .	4
3.2 System Overview . . . . .	5
<b>4 Engineering Design and Analysis</b>	<b>6</b>
4.1 Structural and Mechanical Design . . . . .	6
4.2 Manufacturing and Prototyping . . . . .	7
4.3 Thermal Considerations . . . . .	8
4.4 Propellant Transfer Validation . . . . .	8
4.5 AI Movement and Docking System . . . . .	8
<b>5 Technical Management</b>	<b>9</b>
5.1 Risk Assessment and Mitigation . . . . .	9
5.2 Project Timeline and Budget Estimate . . . . .	9

## 1 Executive Summary

Future lunar missions depend on efficient cryogenic propellant transfer to enable long-duration exploration. Current cryogenic fluids, stored at approximately -196°C, can only be maintained for limited durations, posing a challenge for sustained operations [1]. A major hurdle is the efficient and reliable transfer of large quantities of cryogenic fluids in microgravity. Our proposed system, AMCC-AAC, directly addresses this challenge with a reusable, autonomous, and low-loss propellant transfer system. By integrating advanced magnetic coupler designs with computer vision-assisted docking, AMCC-AAC dynamically adjusts its positioning to optimize the docking sequence. LiDAR and camera based sensing enhance accuracy, while a built-in quick-disconnect system mitigates failures by halting transfer and disconnecting in emergencies. This technology is validated through simulation and functional prototyping with real-world testbed data. AMCC-AAC aims to advance sustainable lunar operations by enabling long-term propellant storage and transfer, supporting a continuous human presence on the moon.

## 2 Problem Statement and NASA Relevance

With a renewed focus on sustained lunar exploration, advancing cryogenic propellant technologies is more crucial than ever. NASA's Artemis program and the Gateway lunar space station aim to enable long-term human presence on the Moon, but achieving this goal requires overcoming significant challenges in cryogenic systems [2]. The SpaceX Starship Human Landing System (HLS), responsible for transporting astronauts to the lunar surface, depends on cryogenics such as liquid oxygen (LOX) and liquid methane ( $\text{LCH}_4$ ) to safely do so. However, the capabilities of current cryogenic systems are underdeveloped relative to the needs of the HLS architecture. Addressing this issue requires novel, innovative solutions to ensure the long-term viability of lunar operations and deep-space exploration.

To bridge this technological gap, advancements in Cryogenic Fluid Management (CFM) are essential. CFM is a complex suite of technologies developed by the Space Technology Mission Directorate (STMD) to demonstrate the ability to successfully and adequately store, transfer, and measure cryogenic fluids in space [3]. One specific area of focus in CFM is large-scale autonomous on-orbit propellant transfer. Designing such a system poses unique challenges due to the behavior of cryogenic fluids in microgravity, including fluid sloshing, phase changes, and thermal management issues.

Ensuring reliable and autonomous cryogenic propellant transfer in space requires advancements in sealing technology, flow control, and thermal insulation to prevent losses from leakage and boil-off. Traditional quick-disconnect cryo-couplers, designed for ground-based applications, face significant challenges in space. High sealing friction, wear-induced leakage, and limited reusability are among the most notable [4]. Additionally, existing couplers require precise manual alignment, making them impractical for automated docking in microgravity. To overcome these challenges, next-generation cryo-couplers must incorporate automation, improved sealing mechanisms, and materials engineered for cryogenic durability.

## 3 Proposed Solution and Technical Approach

### 3.1 Main Assumptions

Before we can give a detailed technical plan for creating an autonomous cryo-coupler system, we first must make some reasonable simplifying assumptions. These assumptions aim to make this project both realistic and flexible for future adaptation. First, we must assume that the HLS architecture follows a 1-stage design for descent and ascent. The descent stage will transfer the crew and cargo from Gateway orbit to the lunar surface and the ascent stage will return the crew and collected lunar samples from the lunar surface back to Gateway [5]. Additionally, we assume no more than 4 crew members will be transferred on the HLS [6]. This will become important when calculating the propellant mass transfer necessary for the mission.

We also assume that propellant transfer occurs between two spacecraft or tanks to maximize the system's applicability. For this project, we have selected the SpaceX Starship HLS as the refueling vehicle, meaning the interface must accommodate its round tank geometry [7]. To keep the project scope focused, we assume that propellant flow through the coupler is managed by a separate subsystem (i.e. pressure differential, pump, or tank venting system). While fluid transfer is a critical aspect, our

design is specifically concerned with ensuring a precise and reliable mechanical connection between the two tanks in space.

Additionally, we assume that one tank remains stationary with a fixed-length receiving hose, while the other incorporates a movement system with a variable hose length for alignment. Our design also presumes that Starship has already docked with the receiving spacecraft or tanker, allowing us to concentrate solely on the automation of the coupling mechanism.

### 3.2 System Overview

To enhance CFM capabilities and develop a framework for reusable cryo-couplers in orbit, we propose an autonomous AI-driven active alignment system, integrated with passive magnetic alignment, to enable the safe and reliable transfer of large quantities of propellant to the HLS. AMCC-AAC aims to accomplish the following key objectives:

1. *Achieve repeatable autonomous docking* of the dynamic coupler with a stationary receiver by using both active and passive alignment.
2. *Reduce leakage and boil-off losses* while transferring large quantities of propellant by use of multilayer insulation (MLI), compressive robotic grippers, and advance o-ring sealants.
3. *Enable rapid emergency disconnect* via a magnetic-assisted quick release mechanism to prevent propellant loss and catastrophic damage.

We accomplish these objectives through use of LiDAR, cameras, onboard HLS sensors, and AI algorithms for sensor fusion and interpretation. Figure 1 provides a high level system overview flowchart of the automated alignment process. Once properly connected, several system checks are performed, and other necessary systems—such as power and communications—are linked before transferring fluid.

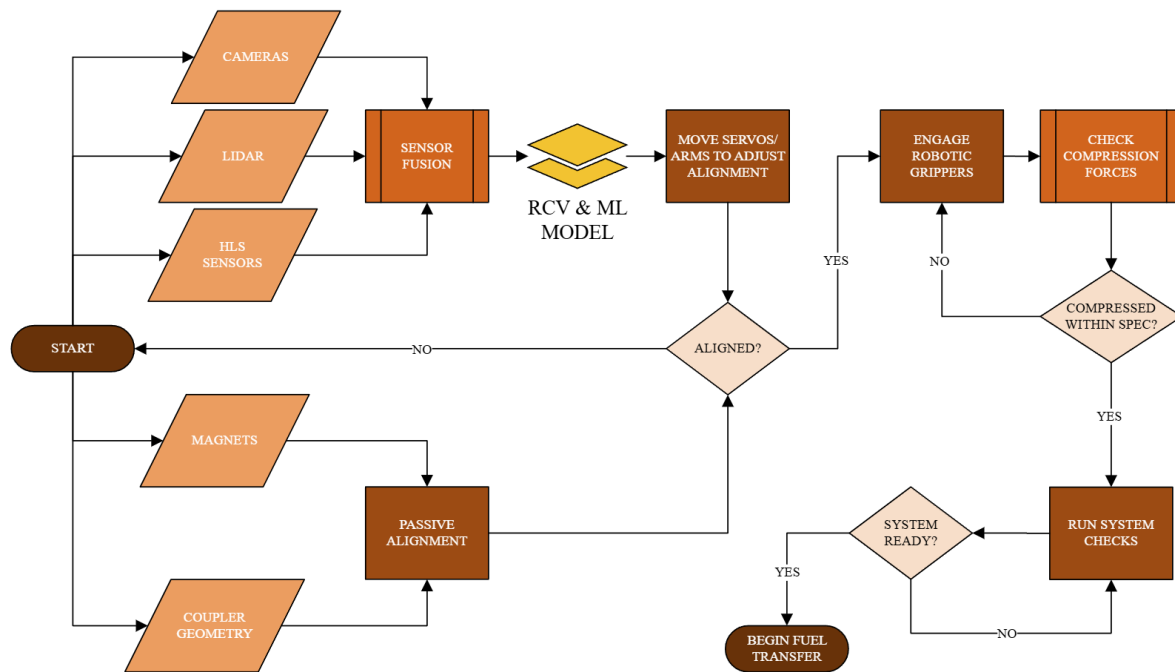


Figure 1: High Level System Overview Flowchart

The emergency disconnect system is a separately developed sub-process that will be integrated with a fluid transfer flowchart. This subsystem will be discussed in more detail below.

## 4 Engineering Design and Analysis

### 4.1 Structural and Mechanical Design

Microgravity and orbital alignment provide challenges that are important to consider when attempting to solve cryogenic fluid transfer. The design of the automated cryo-coupler utilizes several passive and active techniques, as well as specific design considerations to ensure a leak-free seal.

Achieving the goal of repeatable and reliable cryogenic fluid transfer calls for the reduction of static pressure as much as possible within the system's constraints. Specifically, the coupler needs to be able to handle up to 25 kg/s for 12 hours based on the total  $\Delta V$  of 5,400 m/s and mass requirements of 865kg (descent) & 525kg (ascent) for the planned Artemis missions (not including LEO to NRHO where  $\Delta V \approx 9,355$  m/s) [5, 6, 8]. For this reason, an inner diameter of 5 inches has been chosen to accommodate a high mass-flow, low pressure fluid transfer. High mass flow leads to a reduction of lead times and subsequently decreases the risk of leaks. This diameter also allows for cross compatibility with existing plumbing hardware. A preliminary mockup of the internal nozzle geometry is shown in Fig. 2.

After both orbital bodies have approached, establishing the connection between both halves of the coupling is done by robotic movement rods using LiDAR and camera data. The actuation system was modeled based of the ISS Block 1 Docking System illustrated in Fig. 3. Similar to this system, our design uses a direct-drive electromechanical Stewart Platform-based capture system with six independent linear actuators to guide and align the couplers. The plate connection points have been modeled as ball bearings with the option to add more complex joints in the future. Within about 1 inch, the magnets arranged in a radial pattern around each end of the coupling assist both in completing the rest of the displacement and in reinforcing the proper rotation to successfully mate the structure [9]. The angled walls of the nipple and sleeve will accommodate for any micro adjustments needed to guide the couplers into the proper position [10].



Figure 3: Example of ISS Docking System, Image Credit: NASA [11]

not function in Earth temperatures. This topic still requires an in-depth analysis to determine the specific desired tolerancing parameters. However, a preliminary review of manufacturing methods is provided in the next section.

The movement system was designed so that it can be retracted into the conical holder until it is needed. A base plate will need to be added to the Starship HLS outer structure that conforms to its shape. However, the system was designed to only be additive rather than subtractive in terms of parts. No additional components of Starship HLS are compromised by the addition of the AMCC-AAC. The holder contains each of the robotic arms when in the stowed configuration. An example of the movement system fully extended and in a stowed configuration are provided in Fig. 4. Note that the length of the actuators and rods are exaggerated in this concept to better illustrate the detail in each component.

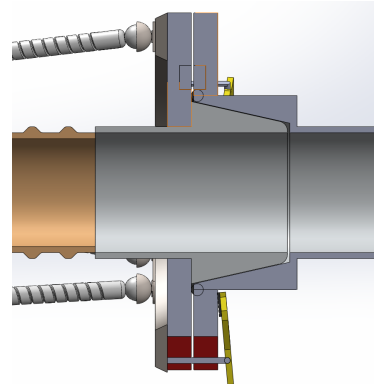
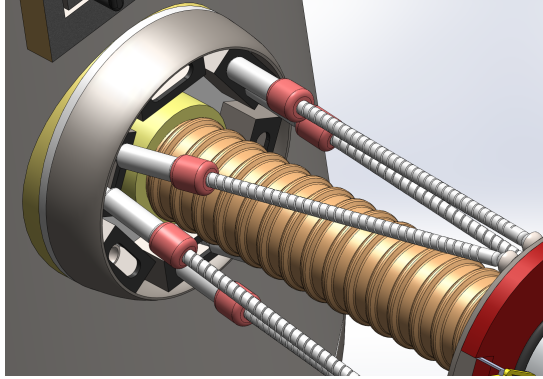


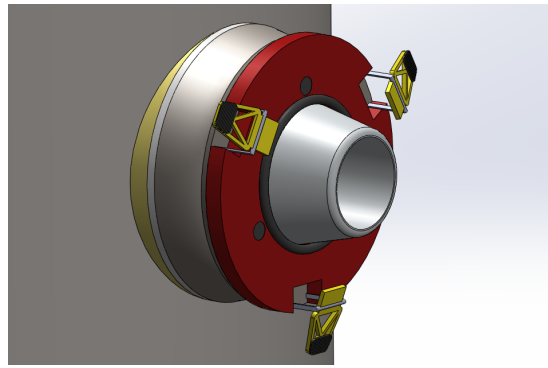
Figure 2: Nozzle Section View.

Once in position, servo arms automatically clamp down and secure the connection between both ends of the coupling. By adding this axial force, the walls of the coupling will reach a minimum tolerance of 0.5mm and the o-ring sitting at the base will be fully engaged, creating a virtually leak-proof seal [12]. To accomplish this, servo selection and testing is vital to ensure the arms and coupling are equipped to handle the loads necessary to fully engage the o-ring.

Tolerancing the coupling is crucial to the function of the final product. A tolerance too loose won't be able to seal properly and expose the fluid to the vacuum of space, but a tolerance too tight won't be able to mate at all. The tolerancing must also account for the thermal contraction of the material, so a coupling designed for space temperatures may



(a) Movement System Extended



(b) Stowed Movement System

Figure 4: The Attachment Plate to HLS with A Extended and Stowed Views

The coupler emergency disconnect will be modeled after the Low Force Disconnect (LFD) system used in the CryoMag at Armstrong Flight Research Center. This system uses equal and opposite load forces applied by the o-ring pressure seals to result in a net zero separation force [13]. Our design implements a similar concept where the low engagement force is easily separated by use of o-rings and retraction of the electromechanical actuators on the movement system. Force tests are the next step to validate this idea, however, the system has proven critical to safely operate a cryo-coupler in the past.

#### 4.2 Manufacturing and Prototyping

The cryo-coupler will be fabricated using Laser Powder Bed Fusion (LPBF), an advanced additive manufacturing (AM) technique that enables complex geometries and minimizes material waste. The primary material, AlSi10Mg, is chosen for its high strength-to-weight ratio, excellent thermal conductivity, and demonstrated performance in cryogenic environments. While this alloy retains mechanical integrity at 20K, its inherent porosity and surface roughness from AM require post-processing to enhance sealing capabilities [14]. Secondary materials, such as Zirconium carbide or Silicon carbide, may be incorporated for additional thermal insulation and wear resistance, while elastomers or metallic gaskets will be used to ensure a vacuum-tight seal.

The manufacturing process begins with design optimization, ensuring the CAD model is tailored for LPBF printing while minimizing post-processing requirements. A polymer prototype (PLA/ABS) will be produced first to assess form and fit before committing to metal fabrication. The final LPBF printing of AlSi10Mg components will be carried out at an AM facility such as The Ohio State University Center for Design and Manufacturing Excellence (CDME). Post-processing will include CNC machining for precision tolerances, heat treatment to enhance mechanical properties, and Hot Isostatic Pressing (HIP) to reduce porosity and improve sealing performance.

Following fabrication, non-destructive testing (NDT) will be conducted to verify structural integrity and performance [15, 16]. Techniques such as X-ray computed tomography (XCT) and dye penetrant inspection will be used to identify defects, while cryogenic leak testing will validate sealing performance under operational conditions [17, 18]. Post-processing and machining will be performed either in-house or outsourced to CDME or B&G Tooling for complex refinements. Material procurement will rely on CDME's (or similar's) vendor network to ensure consistent quality in AlSi10Mg powder and machining tools. Design analysis of the emergency quick disconnect will evaluate latching forces, material durability, and thermal expansion effects to evaluate reliability in cryogenic conditions.

The final development phase will involve subscale prototyping and iterative testing to refine design features before full-scale production. These prototypes will validate mechanical durability, sealing integrity, and quick-release functionality. NASA's stringent standards for long-duration cryogenic propellant transfer will be used to determine validation of the prototypes.

### 4.3 Thermal Considerations

To ensure the structural integrity and functionality of spacecraft components in temperatures ranging from 400K to 50K, a comprehensive thermal management strategy will be implemented [19]. A detailed thermal analysis will map temperature variations across different mission phases, using simulations to model thermal loads and radiation exposure. To mitigate fluctuations, multilayer insulation (MLI) blankets will minimize radiative heat transfer, while low-emissivity coatings control absorption/emission.

Radiation protection will involve shielding with materials such as aluminum and polyethylene to guard against ionizing radiation and high-energy particles. Component placement will be optimized, and radiation-hardened electronics will mitigate single-event effects (SEEs) and total ionizing dose (TID) damage. Structural resilience will be ensured through low-coefficient-of-thermal-expansion (CTE) materials, composite laminates, and thermal barrier coatings. Thermal fatigue testing will verify long-term durability. By integrating these measures, the spacecraft will maintain stable operating conditions and ensure mission success in the extreme cislunar environment.

### 4.4 Propellant Transfer Validation

A validation of leakage and flow requirements will consist of simulation and experimental testing phases. An important assumption that must be made to perform such verifications is that the cryogenic fluid is compressible given a 20kg/s flow requirement. ANSYS Fluent will be used as the primary software for CFD analysis to take advantage of its robust physics modeling in microgravity [20]. Open source CFD code will be used to help simulate flow inside a coupler and then adapted to create a finalized CFD model that is specific to our design. The objectives of the simulation analysis is to analyze the flow behavior through the coupler system, asses the leakage and heat losses, and identify the pressure loss locations.

Simple experimental setups will be used for final prototype validation. Using a fluid that mimics the fluid dynamics of cryogenics at holding temperatures will give the most usable results. Therefore, we plan to use water since studies indicate that the discharge coefficient of water in coupler calibration was similar to most cryogenic fluids within  $\pm 2\%$  uncertainty [21]. While it will not give indications of the thermal properties, it will provide a good understanding of the fluid flowing through our autonomous coupler design.

### 4.5 AI Movement and Docking System

We propose the adoption of an AI-based system to be integrated into the current protocol for cryogenic coupling and in space docking maneuvers. Initially developed for 2D keypoint detection of the ISS docking port, our AI model is being extended to 3D keypoint detection to enhance precision in autonomous docking and cryogenic coupling applications. The existing model, based on a modified MobileNetV3Small Convolutional Neural Network (CNN), has been trained on a dataset that includes depth information, providing spatial awareness. The transition to a Multi-Head Network (MHN) will incorporate this depth as a third dimension, allowing for accurate 3D coordinate prediction. An example, created by our team, of the 2D ISS docking estimation is shown in Fig. 5.

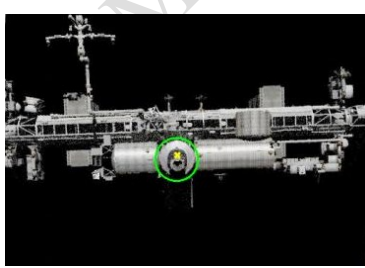


Figure 5: 2D Keypoint of ISS Port Identification Showing Accuracy w/ Clear Image.

This approach aligns with recent advancements in keypoint detection for space applications, where high-resolution networks and online keypoint mining techniques have demonstrated improvements in pose estimation accuracy, particularly in low-visibility conditions [22]. Docking and cryogenic coupling share fundamental requirements, such as precise alignment, secure engagement, and real-time decision-making. Due to these similarities, we pose that our model can be adapted for cryogenic coupling systems.

The computational constraints of space-based systems require efficient AI models capable of real-time inference. Currently, our model processes an image in 80 ms to 1000 ms on a M1 CPU with 8GB RAM. However, modern edge AI accelerators and GPUs can significantly improve inference speeds, with studies showing 5x to 20x improvements over CPU-based infer-

ence [23]. While the specific computational hardware aboard SpaceX's Starship HLS is not publicly available, the spacecraft is designed for autonomous navigation, docking, and lunar operations. Given these capabilities, we can assume the availability of high-performance processors that support AI-driven decision-making [24, 25]. By optimizing our model for these processors, we can ensure fast and reliable real-time performance in mission-critical scenarios.

Rigorous hardware-in-the-loop (HIL) testing in simulated space environments would validate model performance under mission-relevant conditions. These efforts align with NASA's HLS development guidelines, ensuring that our AI system meets safety and reliability requirements for crewed spaceflight operations [26].

## 5 Technical Management

### 5.1 Risk Assessment and Mitigation

Once docked in space, the cryogenic coupler must operate reliably under extreme conditions, with key risks including fluid leakage, thermal contraction, propellant flow instability, and structural degradation. Even minor seal failures can lead to rapid boil-off and hazardous conditions in oxygen-rich environments. To mitigate this, helium mass spectrometry leak detection will be used for pre-deployment screening, while UHV-rated metallic seals and redundant sealing layers will help prevent failures [27]. Additionally, NASA mandates material compatibility testing to minimize flammability hazards in oxygen environments [28]. Vacuum leak testing in ANSYS Fluent will further ensure integrity against this.

Thermal contraction poses another challenge, as extreme temperature fluctuations can cause brittleness and structural stress. Materials with matched CTE will be prioritized, with titanium and stainless steel alloys offering superior low-temperature performance [28]. Cryogenic cycling tests will assess long-term durability in ANSYS Fluent [27]. Additionally, fluid behavior in microgravity can lead to cavitation and pressure spikes, requiring pressure-regulated flow control and real-time sensors to adjust transfer rates dynamically, preventing excessive buildup [29].

Structural degradation from mechanical wear and vacuum conditions must also be addressed. Low-friction coatings and wear-resistant composites will help minimize surface damage, while arc-resistant materials and electrical stress testing in ANSYS Electromagnetic Suite or MATLAB's Partial Differential Equation Toolbox will prevent high-voltage failures [28]. By integrating these strategies, the coupler will maintain structural integrity, minimize failure risks, and ensure safe and efficient operation for long-duration space missions.

### 5.2 Project Timeline and Budget Estimate

To develop and validate the AMCC-AAC system up to TRL 6+, the project will follow a structured timeline spanning approximately 3.5-4 years. This includes coupler design, software development, system integration, and final validation in a relevant environment. A detailed timeline can be viewed in Figure 6 to the right. Key milestones of the project will include:

- *Year 1*: Team assembly, workspace setup, system requirements review, and initial design itera-



Figure 6: Full Project Timeline Overview.

Low-friction coatings and wear-resistant composites will help minimize surface damage, while arc-resistant materials and electrical stress testing in ANSYS Electromagnetic Suite or MATLAB's Partial Differential Equation Toolbox will prevent high-voltage failures [28]. By integrating these strategies, the coupler will maintain structural integrity, minimize failure risks, and ensure safe and efficient operation for long-duration space missions.

### 5.2 Project Timeline and Budget Estimate

To develop and validate the AMCC-AAC system up to TRL 6+, the project will follow a structured timeline spanning approximately 3.5-4 years. This includes coupler design, software development, system integration, and final validation in a relevant environment. A detailed timeline can be viewed in Figure 6 to the right. Key milestones of the project will include:

- *Year 1*: Team assembly, workspace setup, system requirements review, and initial design itera-

tions. Low-level CFD simulations and preliminary design reviews will be conducted.

- **Year 2:** High-level system design, advanced CFD simulations, and prototyping of the coupler. Critical design review and fabrication will take place, followed by microgravity flow testing.
- **Year 3:** Software integration, AI model training, and system validation through simulated and hardware-in-the-loop testing. Pre-integration review will be conducted before final assembly.
- **Year 4:** Final system validation, microgravity testing, and software demonstration to NASA. The project will conclude with a comprehensive report and recommendations for future development.

In terms of short term goals, our team plans to have a low fidelity functional prototype to demonstrate our designs capabilities at the HuLC forum. Simulations will be the primary media used to validate the product during this phase. After the forum, the work outlined would be mostly in scaling the design to a production level quality.

The project budget is structured to support the future 4 year implementation timeline, ensuring the availability of personnel, hardware, and software resources. The total estimated cost is \$6,769,156, which includes salaries, hardware, and software expenses. Major cost breakdowns include:

- **Salaries:** \$6,058,500 allocated for engineers, admins, and technicians for the project duration.
- **Hardware:** \$438,156 for coupler materials, manufacturing, sensors, and testing consumables.
- **Software:** \$272,500 for computers, MATLAB, ANSYS Fluent, SolidWorks, and cloud storage.

The following list of subteams will makeup the required domain of expertise: CAD, CFD, Manufacturing, Space Env. & Human Factors (HF), Thermodynamics, and AI/Robotics. Each subteam will have a lead project engineer, with the remaining members being junior engineers. Figure 7 illustrates the number of engineers allocated to each subteam (including leads) and their expected participation in full-time equivalent (FTE) weeks. The project will include one admin staff to manage logistics and assist with daily non-engineering tasks, as well as one technician serving in a floating role. The proposed resource distribution amounts to 3,718 FTE weeks in total. A cost margin of around ± \$500,000 was used when considering the overall cost range. Adding in this cost margin, the budget range is approximately \$6M to \$7.2M for project completion. Note that this budget is for the future 3-5 year implementation costs imposed on NASA, if the project were to commence. The proposed budget is not the costs associated with the proposal (i.e. the cost to manufacture a low fidelity prototype, train AI, etc.).

Category	Cost				Notes		
	Amount	Unit	Unit Cost	Total Cost			
		FTE (Weeks)	FTE (Weeks)				
<b>A. Salaries</b>							
Project Director	1	employee	182.0	182.00	Will be required throughout project duration		
CAD Engineers	3	employee	182.0	546.00	Will be required throughout project duration		
CFD Engineers	2	employee	182.0	364.00	Will be required throughout project duration		
Manufacturing Engineers	4	employee	182.0	728.00	Will be required throughout project duration		
Space Environment/HF Specialist	1	employee	104.0	104.00	Will only be required for the 1st phase of design		
Thermodynamics Engineers	2	employee	182.0	364.00	Will be required throughout project duration		
AI/Robotics Engineers	3	employee	182.0	546.00	Will be required throughout project duration		
Test Engineers (System Validation)	3	employee	104.0	312.00	Only needed for last 2 years of testing/validation		
Software Engineers (Controls/UI)	2	employee	104.0	208.00	Needed for UI dev. For around 2 years		
Administrative/Technicians	2	employee	182.0	364.00	Will be required throughout project duration		
<b>Salaries Total:</b>	<b>23</b>	, employees		<b>3718.00</b>	, total salary FTE weeks over 3.5 years		
<b>B. Hardware</b>							
	USD (\$)	USD (\$)					
Thermal Insulation (MLI)	165	sqft	800.00	132000.00	MLI including custom fab. (20+ layers)		
Coupler Materials (AlSi10Mg)	200	\$/kg	60.00	12000.00	Materials for prototyping, testing, and extra		
Coupler Casing (Titanium)	70	\$/kg	400.00	28000.00	Materials for prototyping, testing, and extra		
Laser Powder Bed Fusion (LPBF)	20	\$/hr	175.00	3500.00	LPBF machine and facility usage for all phases		
Manufacturing Post-Processing	1	\$	1000.00	1000.00	Additional costs incurred during post-processing		
LiDAR Sensors	3	\$	2000.00	6000.00	1 for prototyping, 1 for final design tests, and 1 backup		
Cameras	3	\$	350.00	1050.00	1 for prototyping, 1 for final design tests, and 1 backup		
Liquid Methane	100	\$/ton	400.00	40000.00	33 cycles of 2.5 min at <20kg/s (if not reused)		
Liquid Oxygen	100	\$/ton	271.06	27106.00	34 cycles of 2.5 min at <20kg/s (if not reused)		
Movement System (servos, robotics)	1	\$	150000.00	150000.00	Entire movement system (minus sensors & cameras)		
Electronics	1	\$	35000.00	35000.00	Additional on-board chips, wiring, batteries, etc.		
Miscellaneous	1	\$	2500.00	2500.00	Additional expenses like repairs/tools/etc.		
<b>Hardware Total</b>				<b>\$ 438,156.00</b>	, total hardware cost over 3.5 years		
<b>C. Software</b>							
	USD (\$)	USD (\$)					
MATLAB/Simulink	3.5	years	5000.00	17500.00	License with some add-ons required for 3 years		
ANSYS Fluent	3	years	65000.00	195000.00	Enterprise CFD license for 3 years		
Computers	5	computers	5000.00	25000.00	Computers required for CFD, CAD, and AI software		
Additional Software/Storage Space/Etc.	1	n/a	35000.00	35000.00	Storage ~ \$30k, other softwares for AI, sensing, etc.		
<b>Software Total</b>				<b>\$ 272,500.00</b>	, total software cost over 3.5 years		
<b>Total Cost (w/o salaries)</b>		<b>FTE (Weeks)</b>	<b>USD (\$)</b>				
		3718.00	\$ 710,656.00				
<b>Total Cost (w/ salaries)</b>		<b>Salaries (\$)</b>	<b>Total (\$)</b>				
		\$ 6,058,500.00	<b>\$ 6,769,156.00</b>				
<b>Estimated Salary Amounts:</b>							
Project Director    Lead Engineer (1 per subteam)    Subteam Engineer    Administrative (1)    Technician (1)							
\$ 180,000.00    \$ 140,000.00    \$ 105,000.00    \$ 78,000.00    \$ 83,000.00							

Figure 7: Detailed Future Program Budget Estimate of AMCC-AAC for 3-5 Year Implementation.

## References

- [1] R. Patterson, A. Hammoud, and M. Elbuluk, "Assessment of Electronics for Cryogenic Space Exploration Missions," *Cryogenics*, vol. 46, no. 2, pp. 231–236, 2006, 2005 Space Cryogenics Workshop. [Online]. Available: <https://www.sciencedirect.com/science/article/pii/S0011227505001736>
- [2] "Gateway Space Station - NASA," <https://www.nasa.gov/reference/gateway-about>, 2023.
- [3] T. Kortes, "Explore Space Tech - Technology Drives Exploration," [https://www.nasa.gov/wp-content/uploads/2015/03/kortes\\_perseverancecfm\\_tagged.pdf](https://www.nasa.gov/wp-content/uploads/2015/03/kortes_perseverancecfm_tagged.pdf), March 2015.
- [4] T. M. Brown, M. Fazah, M. Allison, and H. Williams, "NASA Marshall Space Flight Center In-Space Cryogenic Propulsion Capabilities and Applications To Human Exploration," in *71st JANNAF Propulsion Meeting*, 2024.
- [5] "Human Landing System Requirements Document," NASA, Tech. Rep. HLS-RQMT-001, September 2019.
- [6] K. Latyshev, N. Garzaniti, E. Crawley, and A. Golkar, "Lunar Human Landing System Architecture Tradespace Modeling," *Acta Astronautica*, 2021. [Online]. Available: <https://hdl.handle.net/1721.1/133978>
- [7] "SpaceX – Starship," <https://www.spacex.com/vehicles/starship/>.
- [8] I. Eagle Engineering, "Spacecraft Mass Estimation Relationships and Engine Data," NASA Johnson Space Center, Tech. Rep. 87-171, April 1988, prepared under NASA Contract NAS 9-17878.
- [9] N. Heersema, *Magnetically Latching Cryogenic Fluid Coupler for Lunar Surface Operations*. American Institute of Aeronautics and Astronautics, January 2024. [Online]. Available: <https://arc.aiaa.org/doi/abs/10.2514/6.2024-2371>
- [10] C. Sampaio, "Space Station Freedom Coupling Tasks: An Evaluation of Their Space Operational Compatibility," *Fourth Annual Workshop on Space Operations Applications and Research*, January 1991.
- [11] T. W. R. Justin McFatter, Karl Keiser, "NASA Docking System Block 1: NASA's New Direct Electric Docking System Supporting ISS and Future Human Space Exploration," *Aerospace Mechanisms Symposium*, May 2018.
- [12] R. F. Robbins and P. R. Ludtke, "Review of Static Seals for Cryogenic Systems," *Journal of Spacecraft and Rockets*, vol. 1, no. 3, pp. 253–259, 1964. [Online]. Available: <https://doi.org/10.2514/3.27636>
- [13] "NASA's Low Separation Force Quick Disconnect Device Webinar," <https://www.youtube.com/watch?v=2hICzKjxiu0&t=1s>, June 2022.
- [14] J. G. Santos Macías, Z. Lv, D. Tingaud, B. Bacroix, G. Pyka, C. van der Rest, L. Ryelandt, and A. Simar, "Hot isostatic pressing of laser powder bed fusion alsi10mg: parameter identification and mechanical properties," *Journal of Materials Science*, vol. 57, 06 2022.
- [15] J. Rao, S. L. Sing, P. Liu, J. Wang, and H. Sohn, "Non-destructive testing of metal-based additively manufactured parts and processes: a review," *Virtual and Physical Prototyping*, vol. 18, no. 1, p. e2266658, 2023. [Online]. Available: <https://doi.org/10.1080/17452759.2023.2266658>
- [16] C. Lapre, D. Brouczek, M. Schwentenwein, K. Neumann, N. Benson, C. R. Petersen, O. Bang, and N. M. Israelsen, "Rapid non-destructive inspection of sub-surface defects in 3d printed alumina through 30 layers with 7 μm depth resolution," 2024. [Online]. Available: <https://arxiv.org/abs/2403.17662>

- [17] A. Thompson, D. McNally, I. Maskery, and R. K. Leach, “X-ray computed tomography and additive manufacturing in medicine: a review,” *Int. J. Metrol. Qual. Eng.*, vol. 8, p. 17, 2017. [Online]. Available: <https://doi.org/10.1051/ijmqe/2017015>
- [18] A. Ziabari, S. V. Venkatakrishnan, and Z. Snow, “Enabling rapid x-ray ct characterisation for additive manufacturing using cad models and deep learning-based reconstruction,” *NPJ Computational Materials*, vol. 9, 2023. [Online]. Available: <https://doi.org/10.1038/s41524-023-01032-5>
- [19] P. Clark, “Cubesats in Cislunar Space,” *Small Satellite Conference*, 2018.
- [20] “The Exploration Company Leverages Ansys to Promote Sustainability in Space,” ANSYS, April 2024.
- [21] R. Radebaugh, *Cryogenic Measurements*. John Wiley & Sons, Ltd, 2016, ch. 61, pp. 2181–2224. [Online]. Available: <https://onlinelibrary.wiley.com/doi/abs/10.1002/9781119244752.ch61>
- [22] J. Xu, B. Song, X. Yang, and X. Nan, “An Improved Deep Keypoint Detection Network for Space Targets Pose Estimation,” *Remote Sensing*, vol. 12, p. 3857, 11 2020.
- [23] D. K. Vohra, “Optimising AI Inference for Performance and Efficiency,” 2023.
- [24] T. H. Park and S. D’Amico, “Bridging Domain Gap for Flight-Ready Spaceborne Vision,” 2024. [Online]. Available: <https://arxiv.org/abs/2409.11661>
- [25] M. Bussolino, “Multispectral Vision-Based Relative Navigation to Non-Cooperative Spacecraft,” Master’s thesis, School of Industrial and Information Engineering, Department of Aerospace Science and Technology Politecnico Milano, 2023.
- [26] “Human Landing Systems Development,” <https://www.nasa.gov/reference/human-landing-systems/>, NASA, 2023.
- [27] “Standard Test Method for Calibration and Operation of the Falex Block-on-Ring Friction and Wear Testing Machine,” vol. 05.01, no. D2714-94R19, p. 4, 2024.
- [28] “Standard Materials and Processes Requirements for Spacecraft,” NASA, Tech. Rep. NASA-STD-6016A, 2016.
- [29] M. hee Kim, J. Wilson, F. Cucinotta, L. Simonsen, W. Atwell, F. Badavi, and J. Miller, “Contribution of High Charge and Energy (HZE) Ions During Solar-Particle Event of September 29, 1989,” NASA, 07 1999.